Astronomy & Astrophysics manuscript no. 6383
February 5, 2008

© ESO 2008

arXiv:astro-ph/0611844v1 28 Nov 2006

The millimetre variability of M81*

Multi-epoch dual frequency mm-observations of the nucleus of M81

R. Schödel[1], M. Krips[2], S. Markoff[3], R. Neri[4], and A. Eckart[1]

[1] I. Physikalisches Institut, Universität zu Köln, Zülpicher Str. 77, D-50937 Köln, Germany
e-mail: `rainer@ph1.uni-koeln.de,eckart@ph1.uni-koeln.de`
[2] Harvard-Smithsonian Center for Astrophysics, SMA project, 645 North A'ohoku Place, Hilo, HI 96720
e-mail: `mkrips@cfa.harvard.edu`
[3] Sterrenkundig Instituut "Anton Pannekoek ", Universiteit van Amsterdam, Kruislaan 403, 1098 SJ Amsterdam, The Netherlands
e-mail: `sera@science.uva.nl`
[4] Institut de Radio Astronomie Millimétrique, 300 rue de la Piscine, Domaine Universitaire, 38406 Saint Martin d'Hères, France
e-mail: `neri@iram.fr`

Received September ; accepted

ABSTRACT

Aims. There are still many open questions as to the physical mechanisms at work in Low Luminosity AGN that accrete in the extreme sub-Eddington regime. Simultaneous multi-wavelength studies have been very successful in constraining the properties of Sgr A*, the extremely sub-Eddington black hole at the centre of our Milky Way. M81*, the nucleus of the nearby spiral galaxy M81, is an ideal source to extend the insights obtained on Sgr A* toward higher luminosity AGN. Here we present observations at 3 and 1 mm that were obtained within the framework of a coordinated, multi-wavelength campaign on M81*.
Methods. The continuum emission from M81* was observed during three epochs with the IRAM Plateau de Bure Interferometer simultaneously at wavelengths of 3 and 1 mm.
Results. We present the first flux measurements of M81* at wavelengths around 1 mm. We find that M81* is a continuously variable source with the higher variability observed at the shorter wavelength. Also, the variability at 3 and 1 mm appears to be correlated. Like Sgr A*, M81* appears to display the strongest flux density and variability in the mm-to-submm regime. There remains still some ambiguity concerning the exact location of the turnover frequency from optically thick to optically thin emission. The observed variability time scales point to an upper size limit of the emitting region of the order 25 Schwarzschild radii.
Conclusions. The data show that M81* is indeed a system with very similar physical properties to Sgr A* and an ideal bridge toward high luminosity AGN. The data obtained clearly demonstrate the usefulness and, above all, the necessity of simultaneous multi-wavelength observations of LLAGN.

Key words. LLAGN – mm-observations – galactic nucleus

1. Introduction

At high accretion rates onto black holes, the infall of gas and dissipation of energy via mostly thermal processes in a thin disk are fairly well understood in general terms. In contrast, there is still great debate about which physical mechanisms are dominant in objects which are accreting at well below the Eddington rate. The most extremely sub-Eddington source currently accessible to observations that allows still reasonable statistics for modelling the accretion/emission mechanisms is the central supermassive black hole of our Galaxy, Sagittarius A* (Sgr A*). Its low luminosity has perplexed theorists for decades, and stimulated the re-emergence of radiatively inefficient accretion flow models (RIAFS, see Melia & Falcke 2001; Quataert 2003), including the advection dominated accretion flow model (ADAF, e.g. Narayan & Yi 1994) and its derivatives. These models are characterised by low efficiency in converting thermal energy into electromagnetic radiation, but differ in terms of the inner boundary conditions such as the presence of strong winds (e.g. Blandford & Begelman 1999) and/or convection (Quataert & Gruzinov 1999), each of which lead to differing predictions on the detailed spectral energy distribution (SED) and its variability. Another open question is the role of jets in dissipating accretion energy (e.g. Blandford & Konigl 1979; Falcke & Biermann 1995) and the extent of their contribution to the SED, particularly at higher frequencies (e.g. Falcke & Markoff 2000; Markoff et al. 2001b,a; Yuan et al. 2002). Since jets are observed in almost all accreting astrophysical systems, the importance of jets in weakly accreting systems is a matter of particular interest.

With a luminosity $\sim 10^{-9...-10} \times L_{\rm Edd}$, Sgr A* is – in terms of Eddington luminosity – the weakest accreting black hole with observational statistics good enough to fit models to its spectrum. It is the primary testbed for theoretical models of extreme sub-Eddington accretion, which rely largely on the available radio/submm/NIR/X-ray observations of Sgr A* (for a review see Melia & Falcke 2001). The recent discovery of quiescent and flaring emission from Sgr A* at both X-ray and NIR wavelengths (Baganoff et al. 2001; Genzel et al. 2003; Ghez et al. 2004) has revolutionised our understanding of this particular Low Luminosity Active Galactic Nucleus (LLAGN). The stringent constraints from these data have ruled out several models, leaving only RIAF models, jet models, and combinations thereof

---

Send offprint requests to: R. Schödel

as contenders. Recently, Eckart et al. (2004, 2006) were successful in obtaining the first simultaneous measurements of the emission from Sgr A* at X-ray/NIR wavelengths (with quasi-simultaneous sub-mm observations). These and ongoing coordinated multi-wavelengths campaigns deliver the decisive observations for constraining/eliminating weak accretion models further.

The nearby spiral galaxy M81 (NGC 3031) is an Sb spiral galaxy similar to the Milky Way. It is located at a distance of 3.63 ± 0.34 Mpc (Freedman et al. 1994). Devereux et al. (2003) used spectroscopic measurements of the $H\alpha$ + [N*II*] emission, probably emitted from a rotating gas disk inclined at an angle of $14^\circ \pm 2^\circ$, to infer a mass of $7.0^{+2}_{-1} \times 10^7\,M_\odot$ for the central black hole in M81.

The nucleus of M81, termed M81*, shows typical signs of AGN activity. It has a power-law, variable X-ray continuum (Ishisaki et al. 1996; Page et al. 2004). The X-ray flux from M81 is highly variable, at scales from days to years (La Parola et al. 2004). The nucleus of M81 displays double peaked, broad $H\alpha$ emission lines (Bower et al. 1996). However, the overall luminosity and AGN characteristics of M81* are rather weak and the galaxy is classified as a LINER (low-ionisation nuclear emission-line region, e.g. Ho et al. 1996). With a luminosity of the order of $10^{37}\,\mathrm{erg\,s^{-1}}$ in the radio and $10^{40}\,\mathrm{erg\,s^{-1}}$ in the optical/X-ray domains (see, e.g., compilations by Ho et al. 1996; Ho 1999), its luminosity is $< 10^{-5}$ times the Eddington luminosity in any wavelength regime. M81* is therefore counted among the low-luminosity AGN (LLAGN). It shows the typical spectral energy distribution (SED) of this class of sources, that is characterised by the absence of the so-called big blue bump, the ultraviolet excess found commonly in the higher power AGN (e.g. Ho 1999).

At cm-wavelengths, M81* shows large-amplitude variations (factors up to two at 2 cm) with timescales of a few months and weaker changes of the flux density on timescales ≤ 1 day (Ho et al. 1999). Multi-epoch VLBI observations of M81* at ~0.01 pc resolution at 20 epochs over 4.5 yr reveal a stationary core with a variable (on timescales of ~1 yr) one-sided jet of length 1 mas (3600 AU) towards the northeast (Bietenholz et al. 2000). As for the polarisation properties of M81*, circular polarisation was detected at 4.8, 8.4 (Brunthaler et al. 2001), and 15 GHz (Brunthaler et al. 2006), while linear polarisation appears to be absent at these frequencies. This is an intriguing similarity to Sgr A*, where circular polarisation also dominates over linear polarisation at these wavelengths (Bower et al. 1999a,b,c; Aitken et al. 2000; Bower et al. 2003, 2005).

Sakamoto et al. (2001) present observations of the central kiloparsec of M81 at a wavelength of 3 mm in the CO $J = 1 - 0$ line and continuum at 100 pc resolution. They detect molecular gas in a pseudoring or spiral arm at about 500 pc, but no giant molecular cloud within about 300 pc of the nucleus. They find significant intraday variation of the continuum emission from M81*, suggesting an emitting region of ~100 AU.

Reuter & Lesch (1996) obtained a spectrum of M81* from the radio to the mm-regime. They find an inverted spectrum up to 100 GHz. Its flux density can be described well by the law $S_\nu \propto \nu^{1/3} \exp -(\nu/\nu_c)$ with a turnover frequency of $\nu_c = 200\,\mathrm{GHz}$. They point out the remarkable similarity between the spectrum of M81* and Sgr A* and conclude that the same physical mechanisms might operate in both galactic nuclei. Therefore Reuter & Lesch (1996) suggest that M81* may be a by $\sim 10^4$ upscaled version of Sgr A*.

Thus M81* is a unique source for comparison with Sgr A* and more powerful AGN, and constitutes the next logical step after the successful multi-wavelength observations of Sgr A*. With this aim, a coordinated, multi-wavelength campaign took place in the first half of 2005, involving instruments from the X-ray to the radio domain: the Chandra X-ray observatory, the Lick telescope (NIR), the SMA, the Plateau de Bure Interferometer (PdBI), the VLA, and the GMRT. A compilation of all observations and the interpretation of the multi-wavelength data is presented by Markoff et al. (in preparation). A detailed description of all instruments and the related data reduction would overload the multi-wavelength paper. Therefore, some papers are dedicated to the observations with specific instruments. The X-ray emission lines measured in the Chandra observations are discussed by Young et al. (in preparation). In this paper we focus on the three epochs of mm-observations of M81* that were obtained with the PdBI during this campaign.

2. Observations and data reduction

M81* was observed with the PdBI on 24 February, 14-15 July, and 19-20 July 2005. Six antennae were used for the February observations in the B configuration of the PdBI, which provides typical beam sizes around 1.5″ at ~100 GHz and around 0.8″ at ~200 GHz. The July observations were done with five antennae in the more compact D configuration, with typical beam sizes around 5″ at ~100 GHz and 2.5″ at ~200 GHz. All observations are listed in Table 1.

The observations aimed to detect continuum emission from M81*. However, due to good conditions the receivers were tuned to the ^{12}CO $J = 1 - 0$ and $J = 2 - 1$ transitions at 115.3 and 230.5 GHz in the February observations. Thus, it was possible to search for compact CO-emission within ~20″ of the nucleus, while the continuum could be extracted from the line-free channels (The results of the CO-line imaging will be discussed in a forthcoming paper). For greater phase stability in the July observations, an epoch during which the atmosphere at the site contains more water vapour, the receivers were tuned to frequencies of 80.5 and 86.2 GHz at 3 mm and 241.4 and 218.2 GHz at 1 mm.

The sources 3C273 (February), 3C454.3 (July 14-15) and 1741-038 (July 19-20) were used for bandpass calibration. Phase calibration was performed with the sources 1044+719 and 0836+710. Primary flux calibrators to determine the efficiencies of the antennae were the sources 1044+719 for February 23-24 (1.6 Jy at 3 mm/1.1 Jy at 1 mm), 1044+719 (1.8 Jy at 3 mm) and 2200+420 (8.7 Jy at 1 mm) for July 14/15, and MWC349 (1.0 Jy at 3 mm) and 3C454.3 (33.0 Jy at 1 mm) for July 20. The phase calibrators 1044+719 and 0836+710 were used to fit the time-dependent fluctuations of the amplitude for all baselines. Various tests were performed for estimating the uncertainty of the flux calibration, e.g. using different primary flux calibrators and comparing the resulting fluxes of all observed sources. As an additional test, from a comparison of the calibrated fluxes of the sources 0836+710, 1044+719, and MWC349 between the three epochs we estimated the uncertainty of the absolute flux calibration. To provide a quantitative measurement of the data quality, Table 2 lists the ranges of the rms values of the phase and amplitude that were obtained during calibration of these values for the different baselines for each observing epoch. The table also provides values for the estimated uncertainty of the absolute flux calibration at 3 mm and 1 mm. As can be seen, the quality of the February data is highest. The data from 20 July are clearly better than the data from 14/15 July.

Individual scans of 20 min duration were extracted from the calibrated data. Subsequently, a point source was fitted to the resulting UV tables in order to determine the flux of M81* and of

Table 1. Observations of M81* with the PdBI during 2005. $\nu_{3\,\mathrm{mm}}$ is the exact frequency used around 3 mm, $\nu_{1\,\mathrm{mm}}$ the one at a wavelength of 1 mm. $\mathrm{N_{Ant}}$ is the number of antennae, “Config” refers to the antenna configuration used.

Start [UT]	End [UT]	$\nu_{3\,\mathrm{mm}}$ [GHz]	$\nu_{1\,\mathrm{mm}}$ [GHz]	$\mathrm{N_{Ant}}$	Config
24-FEB-2005 01:11	24-FEB-2005 19:45	115.3	230.5	6	Bp
14-JUL-2005 06:50	15-JUL-2005 13:51	80.5	241.4	5	D
19-JUL-2005 23:17	20-JUL-2005 16:07	86.2	218.2	5	D

Table 2. Data quality: The table lists the ranges of the rms values of the phase and amplitude between all baselines for each observing epoch and wavelength. Also, the estimated systematic error of the absolute flux calibration is indicated.

Date	3 mm phase rms [deg]	3 mm amp rms [%]	3 mm absolute	1 mm phase rms [deg]	1 mm amp rms [%]	1 mm absolute
24-FEB-2005	10-20	5-8	≤10%	20-40	11-18	≤15%
14/15-JUL-2005	15-35	8-11	≤15%	40-60	25-30	≤30%
19/20-JUL-2005	12-28	~3	≤15%	30-70	11-18	≤20%

the two calibrators 0836+710 and 1044+719. Fitting Gaussian functions to the UV tables of M81 gave very similar results, with deviations ≤ 5% at 3 mm and ≤ 15% at 1 mm. Due to the larger number of parameters the uncertainties are larger when fitting Gaussians. The general shape of the radio light curves is not affected by the model that is chosen to fit the data. Since M81* is known to be a point-like radio continuum source that shows structure only on scales of 1 milli-arcsecond (Bietenholz et al. 2000), we decided that fitting a point source appears to be the appropriate way to measure the flux density of M81*.

3. Variability of M81* at mm wavelengths

Figure 1 shows the observed millimetre light curves of M81* along with the corresponding data for the two phase calibrators. The scaling has been chosen such that the average flux of each source equals a value of 1 (arbitrary units), with the fluxes of the calibrators shifted for better comparison. Only the error bars of the relative uncertainty are shown. As for the absolute uncertainty of calibration, it would merely shift the curves along the vertical axes and have no influence on the shape of the curves under stable observing conditions. The flux of the calibrator sources should then fluctuate randomly and with small standard deviation around a constant value. This is the case for the 3 mm-data on 24 February and 20 July, while the conditions were less favourable on 14/15 July. In case of the 1 mm-data, the calibrator measurements fluctuate around a stable average on 20 July, they show trends in parts of the data from 24 February (that are, however, significantly smaller and significantly less pronounced than the trend seen in the flux from M81*), and show significant deviations on 14/15 July.

As for the overall quality of the data, it can be best asserted when examining the calibrator sources (see also Tab. 2 for more quantitative information on the data quality). Clearly, the quality of the data is higher at 3 mm than at 1 mm due to the reduced phase stability at the shorter wavelength. The best data were obtained on February 24, when the lower winter temperatures and vapour content of the atmosphere facilitated measurements at 1 mm. The July 20 observations are excellent at 3 mm and still good at 1 mm. Observing conditions were highly variable on 14/15 July, but it was still possible to obtain good data at 3 mm and acceptable ones at 1 mm. However, a large part of the data had to be discarded during calibration so that in total only about 6 hours of usable data were left.

Some variability of the calibrators can be seen in Fig. 1 that may be correlated with the variability of the target. We tried to take this possibility into account by introducing an additional calibration step that forces the flux of the calibrators to be constant (on average). Thus, any possible systematic uncertainties, leading to spurious variability, can be removed. Figures 2 to 4 and all values in Tab. 3 refer to measurements after this final calibration step was applied (uncertainties introduced by the calibration process were taken into account). Generally, the effect of this additional calibration step is minor. It is illustrated for the Feb. 24 data in Fig. 2. Since (quasi)-simultaneous measurements of sufficient quality for both calibrators were not available for all measurements of M81*, there are less data points in some of the plots in Fig. 3 and 4 than in Fig. 1.

The calibrated flux density measurements of M81* at 3 mm and 1 mm are shown in Fig. 3 (only error bars of the relative uncertainty are shown) and the corresponding spectral indices in Fig. 4 (here, the absolute uncertainties of the flux calibration have been taken into account additionally). The spectral index is defined by $S_\nu \propto \nu^\alpha$, where S_ν is the flux density at a given frequency ν. Time averages of the flux densities and spectral indices are listed in Table 3.

We find the following characteristics of the variability of M81* at wavelengths of 3 mm and 1 mm:

- Variability at the two wavelengths appears to be correlated.
- The amplitude of variability is by a factor ~1.5 larger at 1 mm.
- On 14 July, the flux density at 3 mm is a factor of ~3, at 1 mm a factor of ~2 higher than at the other two epochs.
- The spectral index varies between ~0 and ~-0.5 (Fig. 4 and Tab, 3).
- M81* shows intraday variability, with the fastest variability observed between 08 and 12 h UTC on 24 February.

The light curve of February 24 is shown in the upper panels of Fig. 1. The average flux density and its standard deviation is indicated for different sections of the light curve. A $\gtrsim 5\sigma$ decrease can be seen at 3 mm between 7 and 12 UT. It is accompanied by a similar decrease at 1 mm. The February 24 light curves are shown in Fig. 2 after forcing the two calibrator sources to have a constant flux (on average). This additional calibration step does not alter the intrinsic shape of the light curves in a significant way. Therefore the observed intra-epoch variability must have been intrinsic to the source.

An important question is whether the detected variability could be related to polarisation. We can discard this possibility, however, because a) The directions of linear polarisation of the 3 and 1 mm receivers at the antennae of the PdBI are orthogonal. If

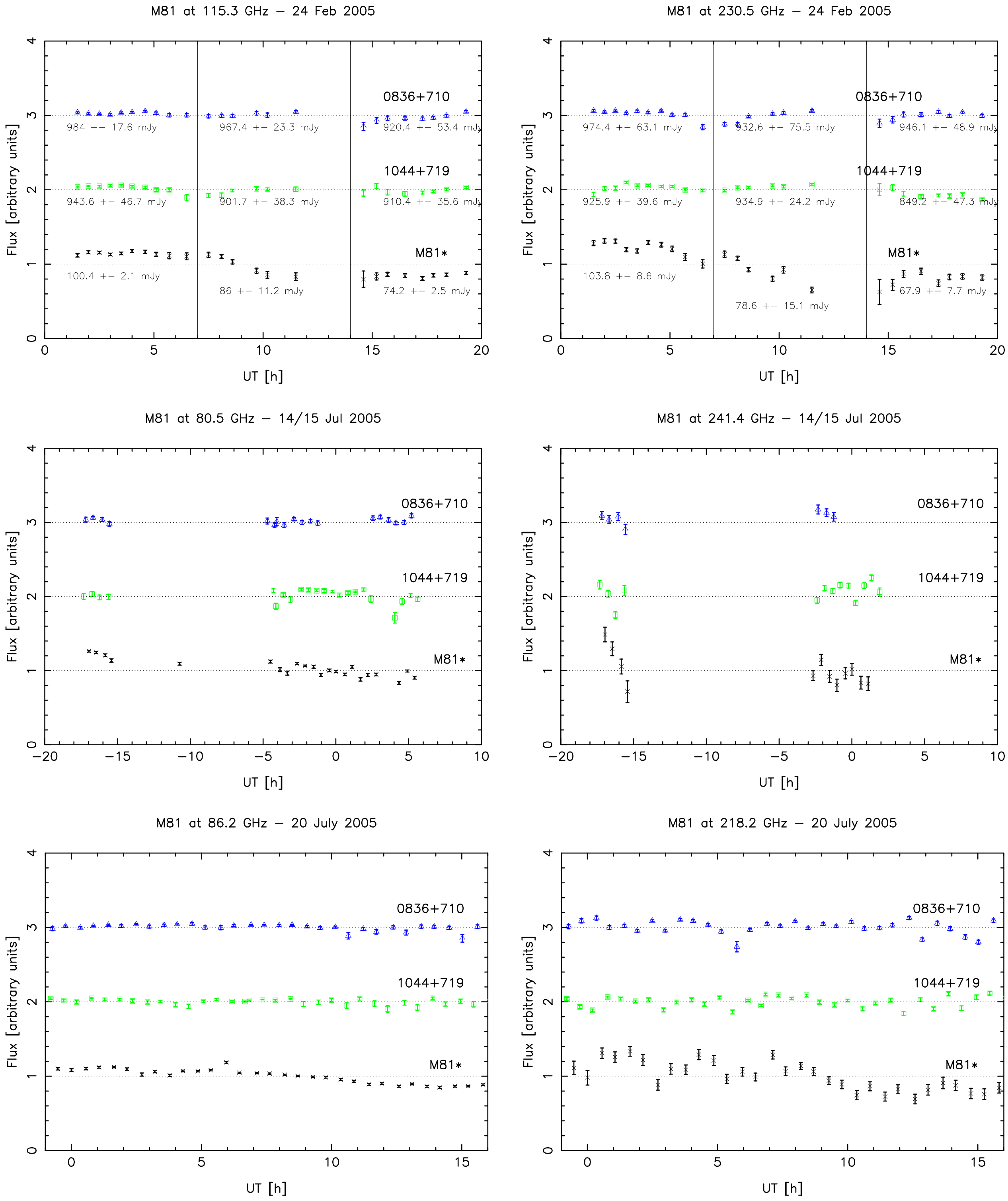

Fig. 1. Light curves of M81* and of the calibrators 1044+719 and 0836+710 from the PdBI observations at 3 and 1 mm. The x-axes show UT in hours. The fluxes were all scaled to an average value of 1, with the curves of the calibrators shifted for better comparison. The vertical lines in the top panels indicate sections for which the average flux and the standard deviation of the individual measurements have been calculated. The corresponding values are indicated.

a sinusoidal pattern due to polarisation were observed at 3 mm, one would expect to observe a similar pattern at 1 mm, shifted by several hours. We do not detect the expected sinusoidal pattern in the light curves nor are the light patterns shifted by several hours in time relative to each other. b) Recent observations of M81* with the BIMA array by Bruntháler et al. (2006) indicate absence of or very low upper limits of a few percent on linear and circular polarisation of M81* at 86 and 230 GHz.

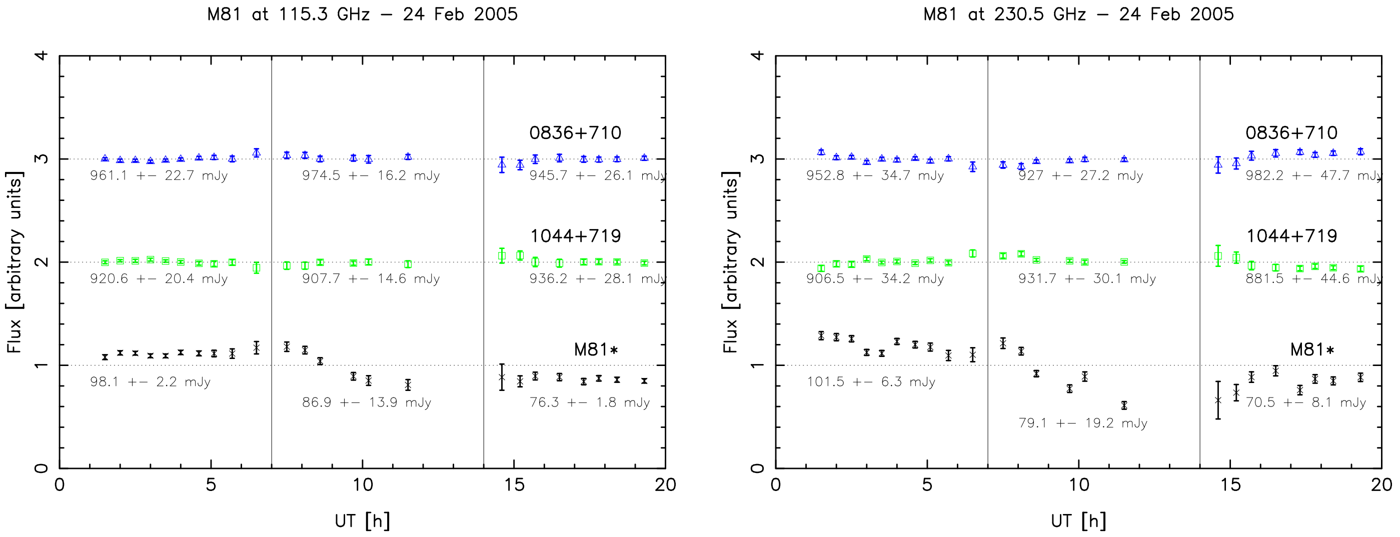

Fig. 2. Light curves of M81* and of the calibrators 1044+719 and 0836+710 from the PdBI observations at 3 and 1 mm on February 24. The light curves were corrected for possible systematic variations by forcing the calibrator sources to have constant flux (on average).

Table 3. Average flux densities of M81*, $S_{3\,\mathrm{mm}}$ and $S_{1\,\mathrm{mm}}$, measured at $\nu_{3\,\mathrm{mm}}$ and $\nu_{1\,\mathrm{mm}}$ during the three epochs of the campaign. The mean and standard deviation (not the error of the mean) were calculated from the unweighted individual measurements shown in Fig. 3. The last column lists the average spectral indices and their standard deviation (not the error of the mean) calculated from all individual measurements as shown in the right panels of Fig. 4.

Start [UT]	End [UT]	$\nu_{3\,\mathrm{mm}}$ [GHz]	$S_{3\,\mathrm{mm}}$	$\nu_{1\,\mathrm{mm}}$ [GHz]	$S_{1\,\mathrm{mm}}$	α
24-FEB-2005 01:11	24-FEB-2005 19:45	115.3	88.0 ± 11.7	230.5	85.6 ± 17.8	−0.06 ± 0.16
14-JUL-2005 06:50	15-JUL-2005 13:51	80.5	241.2 ± 33.8	241.4	181.2 ± 39.1	−0.38 ± 0.17
19-JUL-2005 23:17	20-JUL-2005 16:07	86.2	118.7 ± 11.4	218.2	74.8 ± 13.3	−0.51 ± 0.15

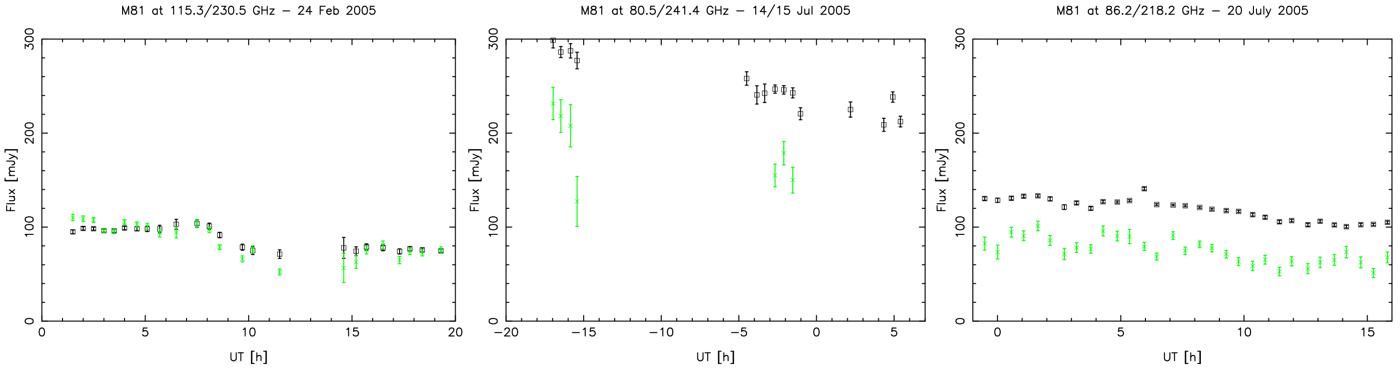

Fig. 3. Flux density of M81* on 24 February, 14/15 July, and 20 July 2005. The black boxes mark the flux density at 3 mm and the green (gray) crosses mark the flux density at 1 mm. The exact frequencies are indicated in the titles of the individual panels. The error bars indicate relative, not absolute, uncertainties.

4. Discussion

Theory and observations indicate that sub-Eddington black holes are jet-dominated (Falcke & Markoff 2000; Falcke et al. 2004; Yuan et al. 2002; Fender et al. 2003). A compact, variable jet has in fact been detected in VLBI observations of M81* (Bietenholz et al., 2000; see also Markoff et al., in preparation). Falcke (1996) demonstrate that a compact jet can explain the observed spectrum of M81* very well. In the jet model, the turnover frequency from a flat (or slightly inverted) radio spectrum to an optically thin power-law occurs at a frequency ν_t. In a simplified model this frequency depends on the jet power, Q_j, and mass of the black hole, M_{BH}, as $\nu_t \propto Q_j^{2/3} M_{\mathrm{BH}}^{-1}$ (Falcke et al. 2004). In LLAGN the turnover occurs generally at (sub)mm wavelengths, while it is located in the near-infrared/optical regime for XRBs in the low/hard state (see Corbel & Fender 2002; Markoff et al. 2003; Falcke et al. 2004).

The simultaneous observations of M81* at 3 and 1 mm presented in this work are consistent with a turnover of the synchrotron emission from a jet in M81* into the optically thin part between 3 mm and 1 mm (with the exception of the first ~4 hours of the 24 February light curve that would indicate a higher turnover frequency). This is in good agreement with the data presented by Reuter & Lesch (1996) that were, however, not acquired simultaneously.

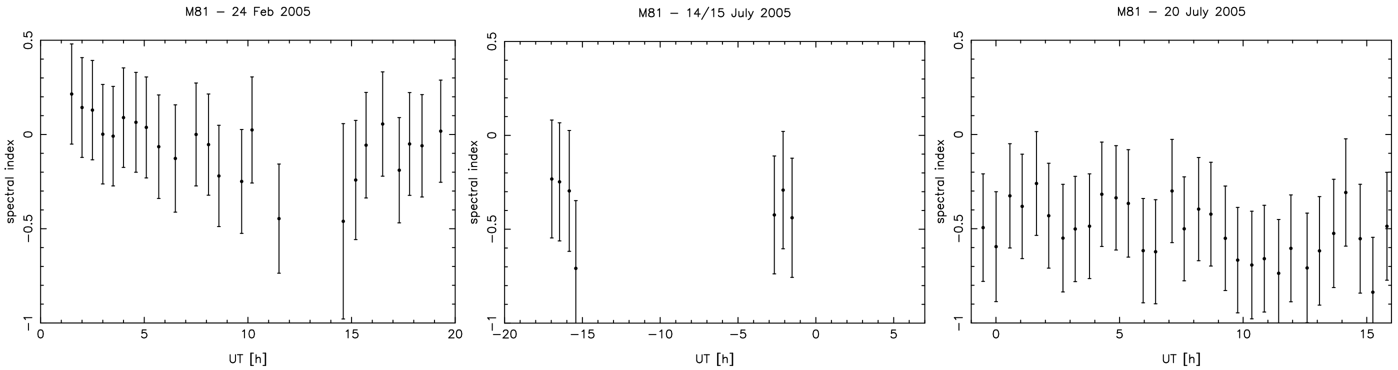

Fig. 4. Spectral index of M81* on 24 February, 14/15 July, and 20 July 2005. The spectral index is defined by $S_\nu \propto \nu^\alpha$, where S_ν is the flux density at a given frequency ν. The absolute uncertainties (see Tab. 2) of the flux densities at 3 and 1 mm have been taken into account for this plot. Since we use upper limits on the absolute uncertainties, the plotted error bars are conservative.

The evidence for the location of the turnover frequency between 3 and 1 mm is ambiguous, however. The multi-frequency radio data from the coordinated campaign indicate that bumps are present in the radio spectrum (Markoff et al., in prep.). These bumps are located at different frequencies at different epochs. Therefore, in spite of the presented mm-data, it may well be possible that there is a submm-bump present in M81*. Observations with the SMA at 345 Ghz that were obtained during the coordinated campaign on M81* indicate that the flux density of M81* increases toward the submm regime, in agreement with theoretical predictions on the existence of a submm-bump (Markoff et al., in preparation). Unfortunately, there was only one epoch (24 February 2005), where measurements with the PdBI and the SMA were simultaneous.

For fine-tuning the models of the emission of M81* it is important to know the exact turnover frequency and whether and how it varies with activity of the source. Therefore there is an urgent need for more observational data for comparison with theory in order to understand sub-Eddington accretion and emission. It is essential that the observations across the wavelength regimes are simultaneous.

Due to the gap of several months there is probably no correlation between the February and July observations because the light curves at 2 cm presented by Ho et al. (1999) indicate that radio outbursts of M81* have generally timescales < 5 months. Also, Sakamoto et al. (2001) have found that M81* shows flux variations **of factors** ≤ 2 at a wavelength of 3 mm on time scales < 10 days. However, the decaying light curve from July 19 may be related to the same event as the light curve on July 14. The spectral index during the two epochs is negative and of similar absolute value (see Tab. 3 and Fig. 4). This behaviour is consistent with a decaying light curve from a low-peaking flare in the model by Valtaoja et al. (1992) that describes variability phenomena in AGN by a growth/decay of shocks in a jet (see also Marscher & Gear 1985).

An estimate of the size scales of the relevant processes can be obtained from the time scales of the observed variability. The drop-off between 07:00 UT and 12:00 UT in the highest quality data set from 24 February 2006 shows that a $\gtrsim 5\sigma$ variability of the flux at 3 mm occurs on a time scale of 5 hours (see also the intraday variability at 3 mm found by Sakamoto et al. 2001). A similarly rapid change of the flux can be seen at 1 mm. Since no signal can travel faster than at the speed of light this corresponds to an upper limit on the size of the source of merely $\sim$25 Schwarzschild radii, when a mass of $7.0 \times 10^7\,M_\odot$ is assumed for the black hole in M81*.

5. Summary

We present three epochs of simultaneous 1 and 3 mm continuum observations of the LLAGN M81* that were obtained in the framework of a coordinated, multi-wavelength campaign (Markoff et al., in preparation).

The observations of M81* with the PdBI at mm-wavelengths confirm that M81* is a continuously varying radio continuum source as has been found previously, mostly at larger wavelengths (see Ho et al. 1999; Bietenholz et al. 2000; Sakamoto et al. 2001). The measurements present the first unambiguous detection of M81* at 1 mm and moreover show that the source is continuously variable at this wavelength as well. The amplitude of the variability is observed to be generally larger at 1 mm than at 3 mm by a factor of roughly 1.5. This agrees well with the trend found by Ho et al. (1999) that the amplitude of the variability increases with frequency in LLAGN. A similar behaviour is found in the far weaker source Sgr A* (e.g. Herrnstein et al. 2004; Miyazaki et al. 2004).

The shortest variability time scales of our observations give upper limits on the size of the emitting region of $\sim$25 Schwarzschild radii, assuming a black hole mass of $7.0 \times 10^7\,M_\odot$.

The decaying light curves observed on 14/15 and on 20 July 2005 may have been related to the same radio outburst. They are consistent with a generalized shock-in jet model (Valtaoja et al. 1992).

The simultaneous measurements of M81* at 3 and 1 mm are consistent with a turnover of the flux in the mm-to-submm regime as predicted by models for a jet dominated source. Some ambiguity remains concerning the exact peak frequency and the related interpretation of variability events.

The observations confirm previous findings that there are many similarities between M81* and Sgr A*, the source related to the supermassive black hole at the center of the Milky Way. This underlines the similarity between LLAGN despite of several orders of magnitudes of difference between their luminosities. M81* can serve as a bridge from the extremely sub-Eddington Sgr A* toward higher luminosity LLAGN. The radio emission from M81* is apparently dominated by a compact jet. The same may be the case for Sgr A*, although such a jet has not yet been discovered due to the strong interstellar scattering toward this source. This work poses a clear case for follow-up observations of the highly sub-Eddington nucleus M81* and for the necessity of simultaneous multi-wavelength observations in general in order to constrain the physical mechanisms in black holes that accrete at rates several orders of magnitude below the Eddington limit.

Acknowledgements. Part of this work was supported by the *Deutsche Forschungsgemeinschaft, DFG* project number 494. We thank Lena Lindt and Jan Martin Winters for their help with the data reduction. Special thanks to M. Nowak fo his efforts in setting up the coordinated campaign on M81.

References

Aitken, D. K., Greaves, J., Chrysostomou, A., et al. 2000, ApJ, 534, L173
Baganoff, F. K., Bautz, M. W., Brandt, W. N., et al. 2001, Nature, 413, 45
Bietenholz, M. F., Bartel, N., & Rupen, M. P. 2000, ApJ, 532, 895
Blandford, R. D. & Begelman, M. C. 1999, MNRAS, 303, L1
Blandford, R. D. & Konigl, A. 1979, ApJ, 232, 34
Bower, G. A., Wilson, A. S., Heckman, T. M., & Richstone, D. O. 1996, AJ, 111, 1901
Bower, G. C., Backer, D. C., Zhao, J., Goss, M., & Falcke, H. 1999a, ApJ, 521, 582
Bower, G. C., Backer, D. C., Zhao, J.-H., Goss, M., & Falcke, H. 1999b, ApJ, 521, 582
Bower, G. C., Falcke, H., & Backer, D. C. 1999c, ApJ, 523, L29
Bower, G. C., Falcke, H., Wright, M. C., & Backer, D. C. 2005, ApJ, 618, L29
Bower, G. C., Wright, M. C. H., Falcke, H., & Backer, D. C. 2003, ApJ, 588, 331
Brunthaler, A., Bower, G. C., & Falcke, H. 2006, A&A, 451, 845
Brunthaler, A., Bower, G. C., Falcke, H., & Mellon, R. R. 2001, ApJ, 560, L123
Corbel, S. & Fender, R. P. 2002, ApJ, 573, L35
Devereux, N., Ford, H., Tsvetanov, Z., & Jacoby, G. 2003, AJ, 125, 1226
Eckart, A., Baganoff, F. K., Morris, M., et al. 2004, A&A, 427, 1
Eckart, A., Baganoff, F. K., Schödel, R., et al. 2006, A&A, 450, 535
Falcke, H. 1996, ApJ, 464, L67+
Falcke, H. & Biermann, P. L. 1995, A&A, 293, 665
Falcke, H., Körding, E., & Markoff, S. 2004, A&A, 414, 895
Falcke, H. & Markoff, S. 2000, A&A, 362, 113
Fender, R. P., Gallo, E., & Jonker, P. G. 2003, MNRAS, 343, L99
Freedman, W. L., Hughes, S. M., Madore, B. F., et al. 1994, ApJ, 427, 628
Genzel, R., Schödel, R., Ott, T., et al. 2003, Nature, 425, 934
Ghez, A. M., Wright, S. A., Matthews, K., et al. 2004, ApJ, 601, L159
Herrnstein, R. M., Zhao, J.-H., Bower, G. C., & Goss, W. M. 2004, AJ, 127, 3399
Ho, L. C. 1999, ApJ, 516, 672
Ho, L. C., Filippenko, A. V., & Sargent, W. L. W. 1996, ApJ, 462, 183
Ho, L. C., van Dyk, S. D., Pooley, G. G., Sramek, R. A., & Weiler, K. W. 1999, AJ, 118, 843
Ishisaki, Y., Makishima, K., Iyomoto, N., et al. 1996, PASJ, 48, 237
La Parola, V., Fabbiano, G., Elvis, M., et al. 2004, ApJ, 601, 831
Markoff, S., Falcke, H., & Fender, R. 2001a, A&A, 372, L25
Markoff, S., Falcke, H., Yuan, F., & Biermann, P. L. 2001b, A&A, 379, L13
Markoff, S., Nowak, M., Corbel, S., Fender, R., & Falcke, H. 2003, A&A, 397, 645
Marscher, A. P. & Gear, W. K. 1985, ApJ, 298, 114
Melia, F. & Falcke, H. 2001, ARA&A, 39, 309
Miyazaki, A., Tsutsumi, T., & Tsuboi, M. 2004, ApJ, 611, L97
Narayan, R. & Yi, I. 1994, ApJ, 428, L13
Page, M. J., Soria, R., Zane, S., Wu, K., & Starling, R. L. C. 2004, A&A, 422, 77
Quataert, E. 2003, Astronomische Nachrichten Supplement, 324, 435
Quataert, E. & Gruzinov, A. 1999, ApJ, 520, 248
Reuter, H.-P. & Lesch, H. 1996, A&A, 310, L5
Sakamoto, K., Fukuda, H., Wada, K., & Habe, A. 2001, AJ, 122, 1319
Valtaoja, E., Terasranta, H., Urpo, S., et al. 1992, A&A, 254, 71
Yuan, F., Markoff, S., & Falcke, H. 2002, A&A, 383, 854